samples, is probably a thermal-remanent magnetization acquired by initial cooling of the lava flows. Within-flow scatter of directions is small, typically smaller than between-site scatter (see Supplementary Information), and the axially symmetric (Fisherian) distribution of virtual geomagnetic poles (Fig. 3e) supports the model that site-means are thermal-remanent magnetizations of geomagnetic secular variation about an axially geocentric dipole field. We find the tilt-corrected, normal-polarity palaeomagnetic pole at 0.5° N, 280.7° E, implying a depositional palaeolatitude of 11 ± 5° for the Griqualand West region. On the seven-point 'Q' scale[32] of reliability, this pole rates a perfect seven.

The low palaeolatitude of the Makganyene diamictite compounds the enigma of Precambrian glaciations. Although glaciogenic deposits of generally Palaeoproterozoic age occur on many cratons, our study provides the first direct and reliable determination of any of these units. It is now documented that both of the broad intervals of Precambrian glaciation, near the beginning and end of the Proterozoic aeon, include glaciogenic sediments deposited in equatorial latitudes. This may indicate a global climate system fundamentally different (due, for example, to changes in Earth's orbital obliquity[33]) from that of the past 500 Myr, when glacial deposits were restricted largely to the polar regions. Alternatively, the low-latitude Precambrian glacial deposits could indicate severe, globally inclusive ice ages (a model called the "Snowball Earth"[34]). In that case, our planet's subsequent recoveries to more mild temperatures would indicate a remarkable resilience to extreme perturbations in climate. □

Received 2 August 1996; accepted 7 January 1997.

1. Hambrey, M. J. & Harland, W. B. *Earth's Pre-Pleistocene Glacial Record* (Cambridge Univ. Press, Cambridge, 1981).
2. Chumakov, N. M. & Elston, D. P. *Episodes* **12,** 115–119 (1989).
3. Embleton, B. J. J. & Williams, G. E. *Earth Planet. Sci. Lett.* **79,** 419–430 (1986).
4. Schmidt, P. W., Williams, G. E. & Embleton, B. J. J. *Earth Planet. Sci. Lett.* **105,** 355–367 (1991).
5. Sohl, L. E. & Christie-Blick, N. *Geol. Soc. Am. Abst. Program.* **27,** A204 (1995).
6. Tankard, A. J. *et al. Crustal Evolution of Southern Africa: 3.8 Billion Years of Earth History* (Springer, New York, 1982).
7. Beukes, N. J. in *Mineral Deposits of Southern Africa* (eds Anhaeusser, C. R. & Maske, S.) 819–828 (Geol. Soc. S. Africa, Johannesburg, 1986).
8. Eriksson, P. G. & Reczko, B. F. F. *J. Afr. Earth Sci.* **21,** 487–504 (1995).
9. Button, A. thesis, Univ. Witwatersrand (1973).
10. Cornell, D. H., Schütte, S. S. & Eglington, B. L. *Precambr. Res.* **79,** 101–123 (1996).
11. Burger, A. J. & Coertze, F. J. *Ann. Geol. Surv. S. Afr.* **10,** 135–141 (1975).
12. Steiger, R. H. & Jäger, E. *Earth Planet. Sci. Lett.* **36,** 359–362 (1977).
13. Trendall, A. F. *et al.* in *3rd Int. Archean Symp.* (eds Glover, J. E. & Ho, S. E.) 81–83 (Geoconferences (W.A.), Perth, 1990).
14. Walraven, F., Armstrong, R. A. & Kruger, F. J. *Tectonophysics* **171,** 23–48 (1990).
15. Briden, J. C. *Phil. Trans. R. Soc. Lond. A* **280,** 405–416 (1976).
16. Hattingh, P. J. & Pauls, N. D. *Precambr. Res.* **69,** 229–240 (1994).
17. Symons, D. T. A. *Geology* **3,** 303–306 (1975).
18. Roy, J. L. & Lapointe, P. L. *Can. J. Earth Sci.* **13,** 749–773 (1976).
19. Morris, W. A. *Geology* **5,** 137–140 (1977).
20. Buchan, K. L., Mortensen, J. K. & Card, K. D. *Precamb. Res.* **69,** 1–10 (1994).
21. Miyano, T. & Beukes, N. J. *Trans. Geol. Soc. S. Afr.* **87,** 111–124 (1984).
22. *Stratigraphy of South Africa* (South African Committee for Stratigraphy, Pretoria, 1980).
23. Beukes, N. J. & Smit, C. A. *S. Afr. J. Geol.* **90,** 378–394 (1987).
24. Eyles, N. *Earth Sci. Rev.* **35,** 1–248 (1994).
25. De Villiers, P. R. & Visser, J. N. J. *Trans. Geol. Soc. S. Afr.* **80,** 1–8 (1977).
26. Visser, J. N. J. thesis, Univ. Orange Free State (1969).
27. Neumiller, C. M. thesis, Northern Illinois Univ. (1990).
28. Visser, J. N. J. *Trans. Geol. Soc. S. Afr.* **74,** 187–199 (1971).
29. Kirschvink, J. L. *Geophys. J. R. Astron. Soc.* **62,** 699–718 (1980).
30. Grobler, N. J. & Botha, B. J. V. *Trans. Geol. Soc. S. Afr.* **79,** 53–57 (1976).
31. Fisher, N. I., Lewis, T. & Embleton, B. J. J. *Statistical Analysis of Spherical Data* (Cambridge Univ. Press, 1987).
32. Van der Voo, R. *Tectonophysics* **184,** 1–9 (1990).
33. Williams, G. E. *Earth Sci. Rev.* **34,** 1–45 (1993).
34. Kirschvink, J. L. in *The Proterozoic Biosphere: A Multidisciplinary Study* (eds Schopf, J. W. & Klein, C.) 51–52 (Cambridge Univ. Press, 1992).

Supplementary Information is available on *Nature's* World-Wide Web site (http://www.nature.com) or as paper copy from Mary Sheehan at the London editorial office of *Nature.*

Acknowledgements. We thank J. Grotzinger, P. Hoffman, R. Powell and D. Sumner for discussions that improved the manuscript; A. J. Kaufman, R. Van der Voo and G. Young for constructive comments; C. Jones for updating the Paleomag program used to analyse palaeomagnetic data; and S. van der Merwe and Samancor for access to subcrop and borehole material at Hotazel and Wessels mines. This work was supported by the FRD in South Africa and the US NSF. D.A.E. was supported by a US NSF graduate research fellowship.

Correspondence should be addressed to D.A.E. (e-mail: devans@gps.caltech.edu).

Seismic image of the subducted trailing fragments of the Farallon plate

Suzan van der Lee* & Guust Nolet

Department of Geosciences, Princeton University, Princeton, New Jersey 08544, USA

The Farallon plate was an enormous oceanic plate located west of the Americas during the Cenozoic and Mesozoic eras. This plate has now been almost completely subducted beneath the American plates. In the Northern Hemisphere, the Farallon plate broke up to form a number of independent smaller plates[1–3] when its western edge approached the North American plate. Here we present a tomographic image of the subducted trailing fragments of the Farallon plate in the upper mantle beneath the western margin of North America. The relatively cold, subducted fragments appear as an intricate region of high seismic S-wave velocity. Comparison of the structure of this high-velocity region with tectonic plate reconstructions and volcanic records enables us to identify individual fragments of the subducted Farallon plate and thus reconstruct qualitatively the kinematic evolution of the Farallon slab in the upper mantle beneath North America.

Relative plate motions of the Pacific, Farallon and North American plates are known from reconstructions based on the magnetic isochrons on the Pacific ocean floor[4,5]. Estimates of the age of the plate on subduction and of the time passed since its subduction have been used to predict the geometry of the subducted Farallon plate beneath North America over time[6]. In addition, the Late Cretaceous and Tertiary record of arc magmatism[7–9] in the western United States provides constraints on the slab geometry and its evolution. This record is commonly explained by a flattening Farallon slab and subsequent slab steepening[2,8,9]. Seismological data can provide important constraints on the slab geometry at depth. Results from early studies and inversions of sparse seismic body-wave travel-time residuals suggest that remnants of the subducted Farallon plate could be located in the upper mantle beneath the western United States[10,11]. More recently, large suites of body-wave travel times have been used to derive lower-mantle images of older subducted material from the Farallon plate[12,13]. Here we present our detailed upper-mantle image of the subducted trailing fragments of the Farallon plate.

We applied the method of partitioned waveform inversion[14,15] to 685 vertical-component broad-band digital seismograms to obtain a three-dimensional image of the S-wave velocity structure of the upper mantle beneath the North American plate. Figure 1 shows the geometry of the wave paths and Fig. 2 shows the resulting three-dimensional image. We suggest that the entire elongated high-velocity anomaly near the western edge of North America (Fig. 2) represents subducted lithosphere from the Farallon plate. The location and coast-parallel trend of the anomaly is consistent with tectonic models of the subducted Farallon plate[6]. The order of magnitude of the S-wave velocity anomaly is also consistent with the expected temperature difference between cold subducted lithosphere and ambient upper mantle, as shown by heat-flow computations for a 60-km thin stalled slab with an initial linear temperature profile from 0 to 1,200 °C (ref. 16). After 26 Myr the temperature anomaly from this slab is still between 200 and 300 °C colder than the surrounding mantle over a region 80 km wide. With an increase

* Present address: Department of Terrestrial Magnetism, Carnegie Institution of Washington, 5241 Broad Branch Road NW, Washington DC 20015, USA.

of ~1% in the S-wave velocity with every 100 °C decrease in temperature[17], the imaged high S-wave velocity anomalies can be explained by material that is presently ~200 °C colder than the ambient upper mantle, which is consistent with our interpretation of the high-velocity anomalies as subducted oceanic lithosphere from the Farallon plate.

In the Northern Hemisphere, two major fragments of the Farallon plate have not yet been entirely subducted. The Juan de Fuca plate is currently subducting beneath the northwestern United States and southwestern Canada, while the Cocos plate is subducting beneath Central America. This present-day subduction has been well studied with local seismic data, which has provided detailed images of subducting slab structure[18,19]. At uppermost mantle depths we also have imaged some high-velocity anomalies related

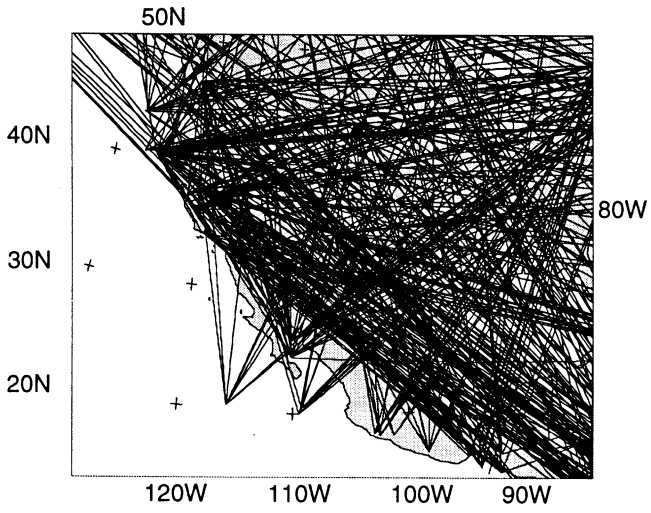

Figure 1 The location, on a map of North America, of the paths travelled by the waves recorded in 685 seismograms. The seismograms are deconvolved with the instrument response to obtain ground displacement records and are windowed around the wave train containing the fundamental and higher-mode Rayleigh waves. The higher modes are sensitive to the structure at deeper levels in the upper mantle, while the fundamental mode is mainly sensitive to the structure of the uppermost mantle. The combination of fundamental and higher modes thus provides good vertical resolution. Good lateral resolution is provided by the large number of wave paths and their wide azimuthal distribution. Synthetic seismograms are computed for a one-dimensional background model that is representative of the average upper mantle between earthquake sources and recording stations. Fine-tuning of the one-dimensional model for each source and receiver pair is performed by fitting the synthetic seismograms to the ground-displacement records with a nonlinear conjugate-gradient optimizer. The resulting path-averaged models are transformed into linear constraints on Earth structure that have uncorrelated errors.

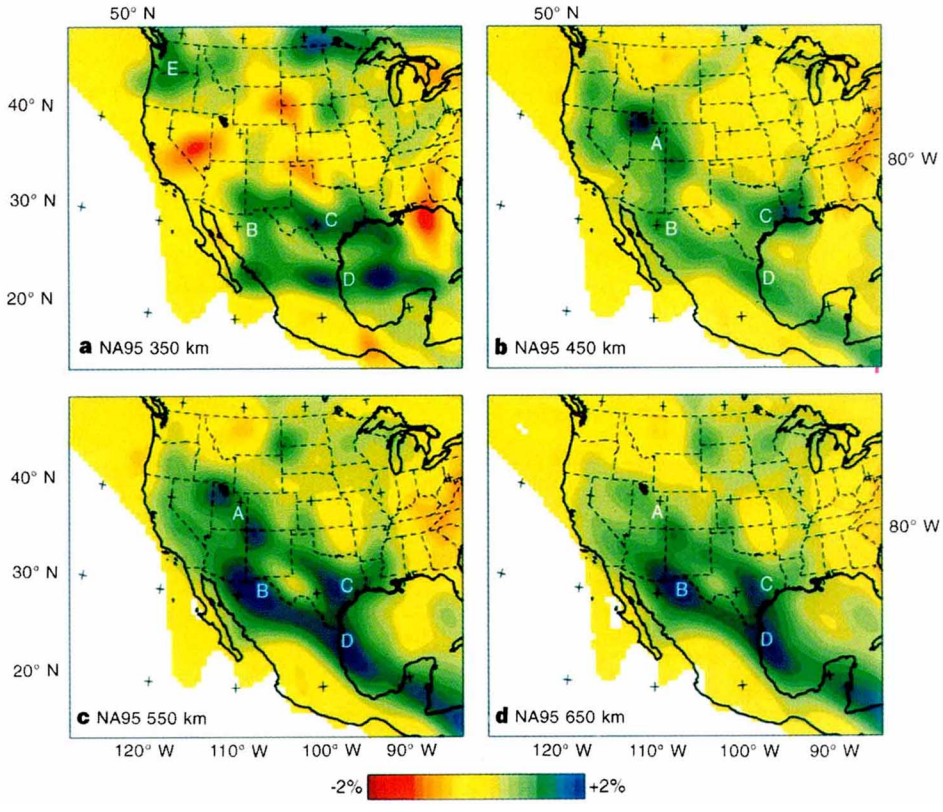

Figure 2 The constraints from all seismograms are combined in a damped linear least squares inversion to yield a three-dimensional model of the S-wave velocity structure of the upper mantle, presented here at different depths, indicated on the maps. Blue and red regions are higher and lower S-wave velocities, respectively. The perturbations are in per cent relative to the background model[26] (see colour scale). The model outlines a complex high-velocity anomaly, which we identify as the Farallon anomaly, beneath the western USA and Mexico just above the transition zone (**a**) and in it (**b**-**d**). The high velocities of the Farallon anomaly are labelled with white letters. The image is robust and resolution tests show that, although the magnitude of the S-velocity anomalies is not well constrained, smooth boundaries of the high-velocity anomaly are spatially resolved to within 200 km (ref. 26). The resolution is best between 15° N and 45° N, although the image is smoothed and the connection between D and B/C may not be real. North of 45° N the resolution degrades at transition-zone depths due to the diminishing sensitivity of the data here. South of 15° N the resolution is less due to degenerating crossing ray coverage (see also Fig. 1). Regions in which the S-wave velocity is not (or poorly) resolved are blanked out.

to the present-day subduction of the Cocos and Juan de Fuca plates, which bracket a region in the uppermost mantle between 18° N and 40° N, without subducted lithosphere. Figure 3 shows a roughly coast-parallel vertical cross-section through our model. In Figs 2 and 3, we have alphabetically labelled the different segments of our image to allow their identification. Based on the positions and trends of the anomalies, we identify anomalies E and D as subducted lithosphere from the subducting Juan de Fuca and the Cocos plates, respectively.

One important feature of our image is the continuous presence, from northwest to southeast, of the Farallon anomaly in the transition zone (Fig. 2b–d). At shallower levels (Fig. 2a) however, anomaly A is missing, thus showing window between anomalies B and C on the southeast side and anomaly E on the northwest side. A window in Farallon subduction started forming 28.5 Myr ago when the Pacific–Farallon ridge first came into contact with North America[2,6]. Hence we conclude that the material from the Farallon anomaly in the transition zone must have subducted before 28.5 Myr ago. the region of the mantle where subducted lithosphere is no longer present is commonly referred to as the slab window. It has been hypothesized that, in the wake of the downgoing slab, the slab window has been filled in with hot low-viscosity mantle material[20,21], generating the Late Oligocene and Miocene record of slab window magmatism[20,22,23]. This hypothesis is consistent with the presence of low S-wave velocities in the region of the slab window at uppermost mantle depths. The vertical cross-section shown in Fig. 3 runs through the slab window and the underlying Farallon anomaly. Relating progressing geological time to decreasing depth, the cross-section shows the onset of slab window formation at 380 km depth (corresponding to 28.5 Myr ago) and subsequent widening, with progressing time and decreasing depth, of the slab window[1,2,6,20,21]. The fact that subducted Farallon lithosphere in this region (anomaly A) reached a depth of 380 km in 28.5 Myr or more, provides an upper bound for the vertical sinking rate of this piece of subducted lithosphere of 1.3 cm yr^{-1}.

A second important feature of our image is the intricate structure of the Farallon anomaly. Although anomalies A, B and C all are roughly parallel to the coastline, they are not located at similar distances perpendicular to the coastline (Fig. 2). In particular, while B and C are located behind each other in a coast-perpendicular direction, they are sharply disconnected from A in a coast-parallel direction. Moreover, while B and C form a pair of two individual coast-parallel anomalies, the coast-side boundary of anomaly A seems less clearly defined as the region between A and the coastline is also of somewhat high S-wave velocity (see, for example, Fig. 2c). to identify anomalies A, B and C we have compared their positions to that of North America, in the fixed-hotspot reference frame[4], during the time of subduction of A, B and C. The position of North America in the period 43–28 Myr ago was several hundreds of kilometers to the northeast of its present-day position[4]. Relative to this position, the boundary between anomalies A and pair B–C is located at the latitude of the present-day northern Gulf of California.

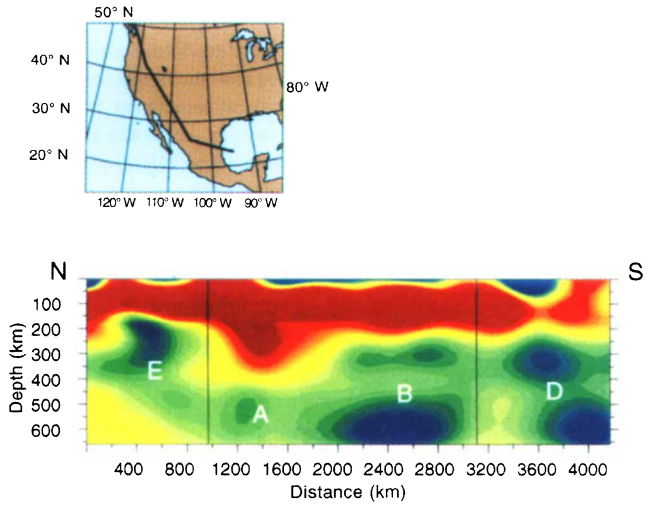

Figure 3 Bottom, vertical cross-section extending from the surface down to the boundary between upper and lower mantle at the 660-km discontinuity. The colour scale is as in Fig. 2. The cross-section is taken along the three combined great circle segments (thick black lines on the accompanying map; top), which follow the trend of the Farallon anomaly.

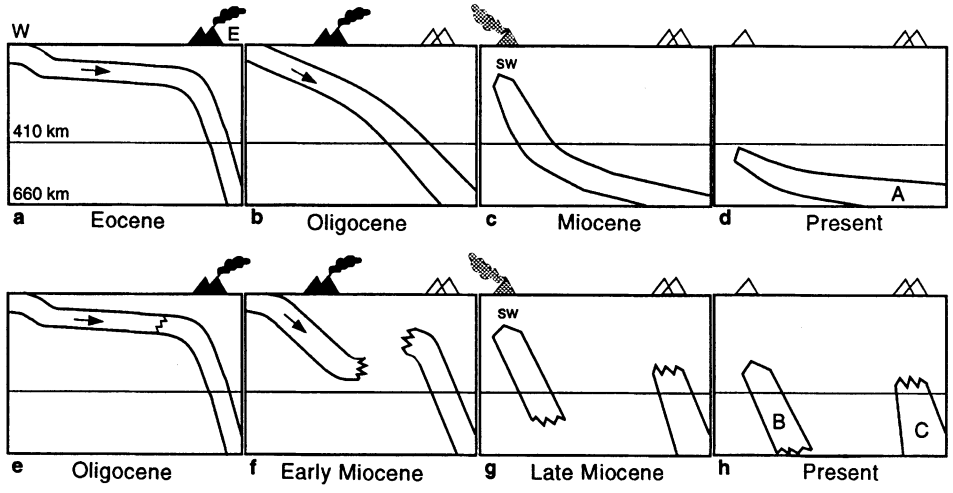

Figure 4 Schematic proposed explanation of the development of anomaly A (**a**–**d**) and anomaly pair B and C (**e**–**h**). Filled triangles represent active volcanism, open triangles represent inactive volcanoes and the arrows denote the direction of subduction. Both developments start with a subhorizontal subducting Farallon slab, where slab flattening has moved arc volcanism (dark shaded triangles) to the east (**a**, **e**). In **b**, the dip angle of the Farallon slab is increasing, which moves the arc volcanism to the west. Once the western edge of the Farallon plate is subducted (**c**), the slab window (sw) in the wake of the subducting Farallon slab initiates slab-window magmatism (light shaded triangles). The slab then further sinks to the transition zone (**d**), which represents our interpretation of high S-wave velocity anomaly A in Fig. 2. Further south, the flat slab breaks and the dip angle of the near-trench part of the slab increases, moving arc volcanism to the west (**f**). In **g**, the two parts of the broken slab continue to sink, the eastern (buoyant) part slower than the western part. In the wake of the subducted western edge of the Farallon plate, the slab window causes magmatism that led to rifting of the Gulf of California. The two parts then sank further into the transition zone (**h**), which represents our interpretation of high S-wave velocity anomalies B and C in Fig. 2.

This corresponds very well with the position 30 Myr ago of the inferred boundary between two major fragments of the Farallon plate, that is, the Vancouver plate to the north, off which the Juan de Fuca plate evolved, and the remainder of the Farallon plate to the south[5]. The Vancouver–Farallon boundary was located very close and parallel, with a roughly ENE strike, to the Mendocino fracture zone, across which the jump in oceanic plate age was extremely large[6].

The far northeastward extent of the region that includes the high velocityies southwest of anomaly A and anomaly A itself, as well as the far northeastward position of anomaly C, strongly suggest that these anomalies were once related to subduction of Farallon lithosphere at very small dip angles. The volcanic record of western North America indicates that subduction indeed occurred at very small dip angles during the beginning (in the north) and the middle (in the south) of the Tertiary, while corresponding arc magmatism occurred as far east as Colorado[2,7–9]. Subsequent increase of the slab's dip angle and westward migration of volcanism, also not simultaneous everywhere, was completed around 20 Myr ago[2,7–9]. A proposed alternative explanation of the volcanic record through downward buckling of the slab[24] cannot be reconciled with our tomographic upper-mantle image.

The mechanism of slab steepening beneath continental lithosphere is not well understood. Here we schematically present (Fig. 4) kinematic models for the evolution of the geometry of the Farallon slab beneath western North America, that are consistent with the volcanic record and our tomographic image. To explain anomaly A and the region of somewhat high S-wave velocities to its southwest, we propose a development as schematically presented in Fig. 4a–d. This development for A is consistent with the western United States volcanic record of westward migrating arc volcanism, followed by slab window magmatism[7–9,20–23]. To explain anomalies B and C we propose a development as schematically presented in Fig. 4e–h. This development for B and C is consistent with the volcanic record[7–9], in particular with the migration of Palaeogene arc magmatism in the Sierra Madre Occidental to Neogene arc magmatism in eastern Baja California and coastal Sonora, which shifted into magmatism related to rifting in the Gulf of California[25] when all trailing Farallon fragments in this region had completely subducted[3]. These fragments have since descended some 350 km in about 16 Myr suggesting an average vertical rate of sinking for this piece of subducted lithosphere of about 2 cm yr^{-1}. □

Received 10 May 1996; accepted 4 February 1997.

1. Atwater, T. Implications of plate tectonics for the Cenozoic tectonic evolution of western North America. *Geol. Soc. Am. Bull.* **81,** 3513–3536 (1970).
2. Atwater, T. in *The Geology of North America* Vol. N, *The Eastern Pacific Ocean and Hawaii* (eds Winterer, E. L., Hussong, D. M. & Decker, R. W.) 21–72 (Geol. Soc. Am., Boulder, CO, 1989).
3. Stock, J. M. & Lee, J. Do microplates in subduction zones leave a geological record? *Tectonics* **13,** 1472–1487 (1994).
4. Engebretson, D. C., Cox, A. & Gordon, A. G. *Relative Motions Between Oceanic and Continental Plates in the Pacific Basin* (Spec. Pap. 206, Geol. Soc. Am., Boulder, CO, 1985).
5. Stock, J. & Molnar, P. Uncertainties and implications of the Late Cretaceous and Tertiary position of North America relative to the Farallon, Kula and Pacific plates. *Tectonics* **7,** 1339–1384 (1988).
6. Severinghaus, J. & Atwater, T. in *Basin and Range Extensional Tectonics Near the Latitude of Las Vegas, Nevada* (ed. Warnicke, B. P.) 1–22 (Mem. 176, Geol. Soc. Am., Boulder, CO, 1990).
7. Lipman, P. W., Protska, H. J. & Christiansen, R. L. Cenozoic volcanism and plate-tectonic evolution of the Western United States. I. Early and Middle Cenozic. *Phil. Trans. R. Soc. Lond. A* **271,** 217–248 (1972).
8. Lipman, P. W. in *The Geology of North America* Vol. G-3, (eds Burchfiel, B. C., Lipman, P. W. & Zoback, M. L.) 481–514 (1992).
9. Cross, T. A. in *Foreland Basins* (eds Allen, P. A. & Homewood, P.) 15–39 (Spec. Publ. 8, Int. Assoc. Sedimentologists, Blackwell Scientific, Oxford, 1986).
10. Solomon, S. C. & Butler, R. G. Prospecting for dead slabs. *Earth Planet. Sci. Lett.* **21,** 421–430 (1974).
11. Romanowicz, B. Large scale three dimensional P velocity strucutre beneath the western U.S. and the lost Farallon plate. *Geophys. Res. Lett.* **7,** 345–348 (1980).
12. Grand, S. P. Mantle shear structure beneath the Americas and surrounding oceans. *J. Geophys Res.* **99,** 11591–11621 (1994).
13. Van der Hilst, R. D., Widiyantoro, S. & Engdahl, E. R. Evidence for deep mantle circulation from global tomography. *Nature* (in the press).
14. Nolet, G. Partitioned waveform inversion and two-dimensional structure under the network of autonomously recording seismographs. *J. Geophys. Res.* **95,** 8499–8512 (1990).
15. Zielhuis, A. & Nolet, G. Shear-wave velocity variations in the upper mantle beneath central Europe. *Geophys. J. Int.* **117,** 695–715 (1994).
16. Davies, J. H. & Stevenson, D. J. Physical model of source region of subduction zone volcanics. *J. Geophys. Res.* **97,** 2037–2070 (1992).
17. Duffy, T. S. & Anderson, D. L. Seismic velocities in mantle minerals and the mineralogy of the upper mantle. *J. Geophys. Res.* **94,** 1895–1912 (1989).
18. Bostock, M. G. & VanDecar, J. C. Upper mantle structure of the northern Cascadia subduction zone. *Can. J. Earth Sci.* **32,** 1–12 (1995).
19. Pardo, M. & Suárez, G. Shape of the subducted Rivera and Cocos plates in southern Mexico: seismic and tectonic implications. *J. Geophys. Res.* **100,** 12357–12394 (1995).
20. Dickinson, W. R. & Snyder, W. S. Geometry of subducted slabs related to San Andreas transform. *J. Geol.* **87,** 609–627 (1979).
21. Dickinson, W. R. Tectonic implications of Cenozoic volcanism in coastal California. *Bull. Geol. Soc. Am.* (in the press).
22. Christiansen, R. L. & Lipman, P. W. Cenozoic volcanism and plate-tectonic evolution of the western United States: II. late Cenozoic. *Phil Trans. R. Soc. Lond. A* **271,** 249–284 (1972).
23. Christiansen, R. L. & McKee, E. H. *Cenozoic Tectonics and Regional Geophysics of the Western Cordillera* (eds Smith, R. B. & Eaton, G. P.) 283–311 (Mem. 152, Geol. Soc. Am., Boulder, CO, 1978).
24. Humphreys, E. D. Post-Laramide removal of the Farallon slab, western United States. *Geology* **23,** 987–990 (1995).
25. Mora-Alvarez, G. & McDowell, F. W. *Miocene Volcanism During Late Subduction and Early Rifting in the Sierra Santa Ursula of Western Sonora, Mexico* (Spec. Pap., Geol. Soc. Am., in the press).
26. Van der Lee, S. & Nolet, G. The upper-mantle *S*-velocity structure of North America. *J. Geophys. Res.* (in the press).

Acknowledgements. We thank the USGS and the IRIS-DMC for making the seismological data available; W. Spakman and colleagues for making available program P, used to make figures 1–3; R. Carlson, M. Debiche, K. Dueker, C. Lithgow-Bertelloni, G. Mora-Alvarez, S. Sacks, P. Silver, J. VanDecar and C. Wolfe for helpful comments. This work was supported by the US National Science Foundation. S.v.d.L. also thanks the Carnegie Institution of Washington for partial support.

Correspondence should be addressed to S.v.d.L. (e-mail: suzan@dtm.ciw.edu).

Hydrostatic locomotion in a limbless tetrapod

James C. O'Reilly*, Dale A. Ritter† & David R. Carrier†‡

* *Department of Biological Sciences, Northern Arizona University, Flagstaff, Arizona 86011-5640, USA*

† *Department of Ecology and Evolutionary Biology, Brown University, Providence, RI 02912, USA*

Caecilians are an ancient and enigmatic group of limbless, burrowing amphibians found throughout most of the humid tropics[1,2]. Over the past 100 million years, the majority of caecilian lineages seem to have retained a series of highly derived musculoskeletal traits from a common ancestor. Among these features are unusually oriented body wall muscles[3] and a vertebral column that moves independently of the skin[4–9]. Until now, these strange characteristics have defied a satisfying functional explanation. Our data suggest that the unique morphology of caecilians enables them to power locomotion hydrostatically by applying force to a crossed-helical array of tendons that surrounds their body cavity. Using this system, the Central American *Dermophis mexicanus* can generate approximately twice the maximum forward force as similar-sized burrowing snakes that rely solely on longitudinally oriented musculature of the body wall and vertebral column for forward force production. Although many groups of invertebrates use hydrostatic systems to move[10–13] and many vertebrates use hydrostatic systems in localized body parts[13,14], caecilians are the first vetebrates known to use the entire body as a hydrostatic system for locomotion.

Because caecilian ribs are not ventrally directed and cannot support their bodies, previous workers have suggested that caecilians maintain body shape during locomotion by means of hydrostatic pressure generated by the unusually vertical muscles of their body wall[3,4,15,16]. To test this hypothesis, we monitored pleuroperitoneal pressures during vigorous locomotion by implanting air-filled catheters in the vestigial left lung of four specimens of *Dermophis mexicanus* and recording pressure changes with a differential pressure transducer. We expected pleuroperitoneal pressure to vary across different modes of locomotion, but to remain fairly constant within each mode. However, to our surprise, in all four subjects pleuroperitoneal pressure varied cyclically during concertina locomotion. In this mode of locomotion, caecilians use movements

‡ Present address: Department of Biology, University of Utah, Salt Lake City, UT 84112, USA.